



The induction of AMPK-dependent autophagy leads to P53 degradation and affects cell growth and migration in kidney cancer cells

Simone Patergnani^a, Sonia Guzzo^b, Alessandra Mangolini^b, Lucio dell'Atti^c, Paolo Pinton^a, Gianluca Aguiari^{b,*}

^a Department of Medical Sciences, Laboratory for Technologies of Advanced Therapies (LTTA), University of Ferrara, via Fossato di Mortara 70 c.o. viale Eliporto, 44121, Ferrara, Italy

^b Department of Biomedical and Surgical Specialty Sciences, University of Ferrara, via Fossato di Mortara 74, 44121, Ferrara, Italy

^c Institute of Urology, University Hospital "Ospedali Riuniti", via Conca 71, 60126, Ancona, Italy

ARTICLE INFO

Keywords:
Kidney cancer
Autophagy
AMPK
p53
Cell growth
MicroRNAs

ABSTRACT

The most common subtype of renal cell carcinoma (RCC) is the clear cell RCC (ccRCC) that accounts for 70–80% of cases. The fate of ccRCC is linked to alterations of genes that regulate *TP53*. The dysfunction of p53 affects several processes including autophagy, which is increased in different advanced carcinomas and could be associated with cancer progression.

We report that different kidney cancer cell lines show higher levels of autophagy than control cells. The increased autophagy is associated with the upregulation of miR501-5p, which stimulates mTOR-independent autophagy by the activation of AMP kinase. AMPK activation occurs through the decrease of ATP generation caused by the downregulation of the mitochondrial calcium uniporter (MCU) that leads to the reduction of mitochondrial calcium uptake. Autophagy induction promotes the degradation of p53 through the autophago-lysosomal machinery. Consistently, the inhibition of autophagy reduces both cell proliferation and migration enhancing the expression of p53, p21 and E-Cadherin as well as decreasing Vimentin synthesis. Taken together, these findings indicate that autophagy is involved in the progression of kidney cancer. Therefore, the pharmacological targeting of this process could be considered an interesting option for the treatment of advanced renal carcinoma.

1. Introduction

Renal cell carcinoma (RCC) is one of the most lethal urological tumors and represents about the 3% of all diagnosed cancers in human [1]. RCC is characterized by different subtypes such as the clear cell RCC (ccRCC) that accounts for ~75% of cases. Others subtypes are the papillary (pRCC) with ~15% of cases, the chromophobe (chRCC) ~5% and the remaining cases (~4%) are not well identified RCC [2]. About one third of ccRCC patients present metastatic disease at time of diagnosis, moreover, the 30% of patients undergoing surgical resection will develop disease recurrence or distance metastases [2]. Most of ccRCC

are associated with *VHL* loss of function, but mutations of others tumor suppressor genes including *CDKN2A*, *TP53*, and *PTEN* seem to be involved in this cancer [3,4]. The tumor suppressor p53 may be degraded by mTOR/MDM2 axis, contributing to cancer metastasis and advanced disease [5]. In this regard, we have reported that the upregulation of miR501-5p induces the activation of mTOR by specific targeting of *TSC1* and leads to the degradation of p53 by the proteasome machinery in ccRCC as well as in autosomal dominant polycystic kidney disease (ADPKD) cells [6,7]. Moreover, also the mutation of *TP53* may correlate with poor survival prognosis in different cancers including ccRCC [8]. It has been reported that p53 deficiency or mutant variants of

Abbreviations: AMPK, AMP-activated protein kinase; ATG7, Autophagy related 7 protein; BECN1, Beclin-1 protein; ccRCC, Clear cell renal cell carcinoma; CDKN2A, Cyclin-dependent kinase inhibitor 2A; EMT, Epithelial mesenchymal transition; HIF, Hypoxia-inducible factor; LC3, Microtubule-associated protein 1A/1B-light chain 3; MCU, Mitochondrial calcium uniporter; MDM2, Mouse double minute 2 homolog; mTOR, Mammalian target of rapamycin; p62/SQSTM1, Sequestosome-1 protein; PTEN, Phosphatase and tensin homolog; RCC, Renal cell carcinoma; TSC1, Tuberous sclerosis 1; ULK1, Unc-51 like autophagy activating kinase; VHL, Von Hippel-Lindau.

* Corresponding author. Department of Biomedical and Surgical Specialty Sciences, University of Ferrara, via Fossato di Mortara 74, 44100, Ferrara, Italy.

E-mail address: dsn@unife.it (G. Aguiari).

<https://doi.org/10.1016/j.yexcr.2020.112190>

Received 30 April 2020; Received in revised form 10 July 2020; Accepted 21 July 2020

Available online 24 July 2020

0014-4827/© 2020 Elsevier Inc. All rights reserved.

p53 protein that accumulate in the cytoplasm of tumor cells were able to activate autophagy [9]. The activation of autophagy may help tumors to maintain energy metabolism to drive their expansion, metastasis, and sustain their survival, contributing to disease progression [10]. To date, the overall survival of patients with metastatic RCC remains under 3 years even though the use of targeted therapies [11]. Therefore, the research of new therapeutic targets is needed to improve the treatment of advanced disease.

2. Material and methods

2.1. Reagents

All media, flasks, tubes, plates, pipettes and other materials for cell culture were bought from EuroClone (Milan, Italy). Anti-P-mTOR (Ser 2448), anti-mTOR, anti-LC3B, anti-ATG7, anti-P-AMPK (Thr 172), anti-AMPK, anti-P-ULK1 (Ser 317), anti-ULK1, anti-E-Cadherin, anti-Vimentin, anti-p53 and anti- β -Actin antibodies were purchased from Cell Signaling Technologies (EuroClone). Anti-Luciferase antibody was acquired from Thermo-Fisher (Monza, Italy), while anti-MCU and anti-p62/SQSTM1 antibodies were obtained from Sigma-Aldrich (Merck, Milan, Italy). Enhanced chemiluminescent substrates for Western blotting and HRP-conjugated anti-rabbit and anti-mouse antibodies were purchased from EuroClone. TurboFect transfecting reagent was obtained from Thermo Fisher Scientific. Rapamycin and compound C (inhibitors of mTOR and AMPK, respectively) were purchased from Sigma-Aldrich. AntagomiR anti-microRNA501-5p was bought from Ambion (Thermo Fisher Scientific), while the plasmid expressing miR501-5p sequences (PL501) was produced by OriGene Technologies (Tema Ricerca, Bologna, Italy). The recombinant p53-GFP construct was kindly gift from Dr. Schimmer (University Health Network, Toronto, Canada), while the oligonucleotides for the silencing of p53 were purchased from Santa Cruz Biotechnologies (D.B.A., Milan, Italy). GFP-LC3 and mCherry-eGFP-LC3 vectors were a gift of Prof. Guido Kroemer and Prof. Paola Rusmini, respectively. MCU-Luc plasmid was prepared as previously reported [12].

This work was in line with the ethical guidelines of the 1975 Declaration of Helsinki.

2.2. Cell lines, proliferation and migration

Embryonic kidney HEK293 cells (ATCC, Manassas, VA, USA) and SW40-transformed normal epithelial kidney 4/5 cells [13] were used as control. Non papillary kidney cancer KJ29 cells were established and characterized as previously described [14], while clear cell renal cell carcinoma (ccRCC) Caki-1 and Caki-2 cell lines were obtained from ATCC. Original cell lines, starved in liquid nitrogen, were resuscitated and cultured up to a maximum of six months at 37 °C in DMEM/F12 (1:1) medium supplemented with 10% FBS by a humidified incubator (95% air-5% CO₂). All cell lines were periodically screened for mycoplasma contamination.

Cell proliferation was analyzed by using the CellTiter method (Promega, Milan, Italy). Briefly, 5000 cells for well were seeded in 96-well plates and starved overnight in DMEM/F12 0.4% BSA. Next, cells were transduced in DMEM/F12 1% FBS for 24 h with either shATG7 lentiviruses able to silence the ATG7 gene or pLKO lentivirus used as control. After transduction, cells were cultured for further 24 h in DMEM/F12 supplemented with 1% FBS and incubated at 37 °C for 5 h with a solution containing tetrazolium salts that were converted by living cells in formazan, a purple compound. Finally, the culture medium was placed in a new 96-well plate and color intensity was measured at 490 nm by a plate reader. The intensity of color is directly proportional to the number of living cells [15].

The analysis of cell migration was performed seeding 30000 KJ29 and Caki-2 cells in 24 well plates. Next, cells were infected with pLKO or shATG7 lentivirus for 24 h in DMEM/F12 medium supplemented with

1% FBS and cultured up to confluence. Finally, a groove between the cells was generated using a sterile tip and cells were grown for further 48 h. Cell migration (groove filling) was analyzed comparing images acquired at T = 0 (empty groove) with those acquired after 48 h of culture by a phase contrast microscope equipped with a CCD camera. The percentage of cell spreading was calculated using the ImageJ software.

2.3. Cell transfection and transduction

Control and cancer cells were transiently transfected by using the non-immunogenic transfection reagent TurboFect (Thermo Fisher Scientific). Before transfection, 200000 cells for well were seeded and cultured overnight in DMEM/F12 medium supplemented with 10% FBS using six well plates. After medium replacement (DMEM/F12 0.4% BSA), cells were transfected for 6 h with either PL501 (1.5 μ g/ml or 3 μ g/ml) expressing miR501-5p sequences or an irrelevant plasmid (control DNA) in combination with p53-GFP, GFP-LC3, mCherry-eGFP-LC3, MCU-Luc and mtLUC constructs (ratio 3:1), as appropriate. The downregulation of miR501-5p was performed transfecting control and tumor cells with 30 nM of anti-miR501-5p sequences (AM). After transfection, cells were washed twice with PBS buffer and cultured for further 24 or 48 h in DMEM/F12 1% FBS and analyzed.

Lentivirus particles were produced transfecting HEK293 cells with recombinant vectors (Sigma-Aldrich) expressing shRNAs for the silencing of the ATG7 gene (shATG7) or with the empty vector used as control (pLKO) in combination with helper plasmids pCMV-dr8.74 and pCMV-VSVG. Briefly, HEK293 cells were seeded at the density of 1.5×10^6 cells/plate by using petri plates (100 \times 20 mm) and cultured until 90% of confluence in DMEM/F12 10% FBS. Next cells were transfected overnight with the plasmids described above by the TurboFect Transfection Reagent and washed twice with PBS buffer. The transfected cells were cultured for further 48 h in DMEM/F12 1% FBS and cell supernatant containing viral particles was collected in sterile tubes. Finally, cell supernatant was filtered by using 0.45 μ m filters (Millipore, Sigma Aldrich) to remove cell debris and used to infect cells or starved at -80 °C. The silencing of ATG7 gene was performed culturing 200000 KJ29 and Caki-2 cells in six well plates overnight in DMEM/F12 10% FBS. After medium replacement (DMEM/F12 1% FBS), cells were transduced with shATG7 and pLKO lentiviruses (medium dilution 1:10) for 24 h. Finally, the medium containing lentivirus particles was discharged and cells were cultured in DMEM/F12 1% FBS for further 24 h.

2.4. Western blotting

Cells were washed twice in PBS buffer containing a cocktail of protease and phosphatase inhibitors (Sigma-Aldrich), detached and collected by centrifugation for 10 min at 800 \times g. Cell pellets were lysed in lysis buffer 1% Triton X-100 supplemented with a cocktail of protease and phosphatase inhibitors. 50 μ g of total protein lysate were electrophoresed in 8% or 12.5% SDS-polyacrylamide gel and transferred onto nitrocellulose membranes (Euroclone). Filters were blocked at room temperature for 1 h in 5% nonfat dried milk PBS-T (PBS with 0.05% Tween 20) and probed overnight at 4 °C in blocking solution containing the specific primary antibody with constant shaking. After three washing in PBS-T, filters were incubated for 1 h at room temperature with the appropriate horseradish peroxidase-conjugated secondary antibody diluted in blocking solution and washed three more times in PBS-T. Next, protein bands were detected by using Super Signal Femto or Pico chemiluminescence systems (Thermo Fisher Scientific). Band images, acquired by film scanning, were processed by ImageJ program. Phosphorylation levels were calculated as ratio between the phosphorylated form and total protein, while the protein content was quantified as ratio between the protein of interest and β -Actin.

2.5. Cell imaging and luciferase assay

Analysis of autophagy was also performed by fluorescence microscopy using GFP-LC3 or mCherry-eGFP-LC3 chimeric proteins. 200000 HEK293 and KJ29 cells were seeded on 24 mm coverslips and cultured overnight in DMEM/12 10% FBS. Next, cells were co-transfected with the PL501 plasmid in combination with GFP-LC3 vector or LC3-mCherry construct for 6 h using the Turbofect reagent (Thermo Fisher Scientific) in DMEM/F12 0.4% BSA and cultured for further 24 h in DMEM/F12 1% FBS. As control, cells were transfected with an irrelevant plasmid instead of PL501 vector. After transfection, cells were washed twice in PBS buffer, fixed at RT in 4% paraformaldehyde for 15 min and permeabilized in 100% methanol for 10 min at -20°C , in order to preserve the autophagic structures. Next, cells were washed twice with PBS buffer, treated for 10 min with a Dapi solution and washed three more times. Images were acquired at $40\times$ magnification using a Zeiss Axiovert 200 fluorescence microscope equipped with a back-illuminated CCD camera (Roper Scientific, Tucson, AZ) and processed by ImageJ software.

The co-localization of p53 protein in autophagosome structures was investigated by fluorescence microscopy in cell transfected with a plasmid expressing wild type p53 linked to GFP and treated with an anti-LC3 antibody able to detect autophagosomes. Briefly, KJ29 and Caki-2 cells, cultured on 24 mm coverslips, were co-transfected with the PL501 construct or control plasmid and p53-GFP recombinant vector (ratio 3:1). After transfection, cells were fixed and permeabilized following the procedure described above. Next, cells were blocked at room temperature for 1 h in PBS 2% BSA and treated with a primary anti-LC3 antibody overnight at 4°C . Finally, cells were washed three times in PBS, treated with a secondary rhodamine-conjugated antibody (Thermo Fisher Scientific) for 1 h and washed again for three times. Images were acquired by a fluorescence microscope at $40\times$ magnification and processed by ImageJ software.

Luciferase assay was performed in HEK293 cells (200000 cells for well) seeded in a six-well plate and cultured overnight in DMEM/F12 medium supplemented with 10% FBS. Next, cells were transfected with the PL501 vector or control plasmid in presence of MCU-Luc (containing the 3' UTR region of MCU mRNA inserted downstream of luciferase gene) and β -galactosidase recombinant constructs (ratio 3:1:1) for 6 h using the Turbofect reagent (Thermo Fisher Scientific) in DMEM/F12 0.4% BSA. After transfection, cells were washed and cultured for further 24 h in DMEM/F12 medium supplemented with 1% FBS. Cells were lysed and an aliquot of protein solution was mixed with luciferase and β -galactosidase substrates in separated tubes following the manufacturer's protocol (Promega). Luciferase and β -galactosidase activity was measured as count number using a 20/20⁺ luminometer (Turner Biosystems, Sunnyvale, CA). Values of luciferase activity were calculated as ratio between counts of luciferase and those of β -galactosidase used for sample normalization [16].

2.6. Mitochondrial calcium and ATP measurements

Cells were seeded onto 13 mm glass coverslips and transfected with the PL501 or control plasmid and the mtAEQ vector expressing the photoprotein aequorin targeted to mitochondria (ratio 3:1). After 24 h, cells were incubated with $5\ \mu\text{M}$ coelenterazine for 1.5 h at 37°C in Krebs-Ringer modified buffer (125 mM NaCl, 5 mM KCl, 1 mM Na_3PO_4 , 1 mM MgSO_4 , 5.5 mM glucose, and 20 mM 4-(2-hydroxyethyl)-1-piperazineethanesulfonic acid [HEPES], pH 7.4, supplemented with 1 mM CaCl_2) and transferred to the perfusion chamber of a luminometer. Next, cell were stimulated with $100\ \mu\text{M}$ ATP diluted in Krebs-Ringer buffer supplemented with 1 mM CaCl_2 and perfused in a hypotonic Ca^{2+} -rich solution (10 mM CaCl_2 in H_2O) supplemented with Triton X-100 in order to discharging the remaining aequorin pool. The light signals was calibrated into Ca^{2+} values, as previously described [17]. Mitochondrial ATP generation was analyzed in cells seeded onto 13 mm

glass coverslips and transfected with the PL501 or control plasmid and a construct expressing the chimeric photoprotein luciferase targeted to the mitochondria (mtLUC). After 36 h, cells were transferred to the perfusion chamber of a luminometer and perfused in Krebs-Ringer buffer supplemented with 1 mM CaCl_2 . Mitochondrial ATP basal content was measured by adding a solution with 1 mM CaCl_2 and 20 mM luciferin, as previously reported [18]. Finally, the light output registered was normalized on the luciferase protein levels detected by immunoblot.

2.7. Analysis of microRNA expression by Real Time RT-PCR

Total RNA was extracted from HEK293 and KJ29 non-transfected cells as well as from KJ29 transfected with the PL501 plasmid, the control vector and with anti-miR501-5p oligonucleotides by TRIZOL transfection reagent (Thermo Fisher Scientific). The synthesis of cDNA was performed by using the Taq-Man MicroRNA Reverse Transcription Kit (Thermo Fisher Scientific). The expression of miR501-5p was evaluated by Real Time RT-PCR using the small nuclear U6B RNA for sample normalization (endogenous control). Quantitative PCR was carried out using the TaqMan method with the Rotor-Gene Q Real time PCR cycler (Qiagen, Milan, Italy). The levels of miR501-5p (target) were obtained by using the ΔCT method, which uses the threshold cycle (CT) number at which the emitted fluorescence of the sample passes a fixed threshold above the baseline. The abundance of the small nuclear U6B RNA was used as endogenous control RNA for sample normalization (reference). The ΔCT was calculated as follows: $\Delta\text{CT} = \text{CT}(\text{target}) - \text{CT}(\text{reference})$. Lower ΔCT values indicate higher amount of target. Thus, the sample with the highest ΔCT that express the lowest amount of miR501-5p is identified as the calibrator (1X expression level) and its value was subtracted from ΔCT values of the other samples to determine the $\Delta\Delta\text{CT}$ value, as shown by the following formula: $\Delta\Delta\text{CT} = \Delta\text{CT}(\text{sample}) - \Delta\text{CT}(\text{calibrator})$. The relative abundance of miR501-5p, expressed as N fold content, was calculated by using the formula $N(\text{target}) = 2^{-\Delta\Delta\text{CT}}$, as previously described [16].

2.8. Statistical analysis

Statistical analysis was performed by using the Anova test or Student's *t*-test, as appropriate. Data are reported as mean \pm standard deviation of at least three independent experiments and differences were considered significant at $p < 0.05$. Statistical significance was calculated by using the GraphPad Prism software. All data used to calculate the statistical significance are inserted in [Supplementary Table 1](#).

3. Results

3.1. MicroRNA501-5p upregulation increases autophagy in kidney cells

The role of autophagy in cancer development and progression is still debated, but it may promote tumor cell survival, migration and invasion [19]. We have found that KJ29, Caki-1 and Caki-2 kidney cancer cell lines exhibited increased levels of LC3-II and reduced expression of p62/SQSTM1 protein compared with 4/5 and HEK293 control kidney cells (Fig. 1A). Consistently, cell transfection with a plasmid expressing LC3 protein linked to GFP produced a greater number of autophagosomes in KJ29, Caki-1 and Caki-2 than in HEK293 cells (Fig. 1B), suggesting that autophagy could affect the fate of renal carcinoma. Previously, we have reported that miR501-5p correlates with tumor progression in kidney cancer [6], therefore it could be involved in the regulation of autophagy. Interestingly, KJ29 tumor cells that show increased autophagy exhibit higher levels of miR501-5p than HEK293 control cells (Fig. 1C). In order to test if the expression of miR501-5p may affect autophagy, it was evaluated in KJ29 cells transfected with a plasmid expressing miR501-5p sequences (PL501), with anti-miR501-5p oligonucleotides (AM) and with an irrelevant plasmid used as control (CTRL). The transfection of KJ29 cells with the PL501

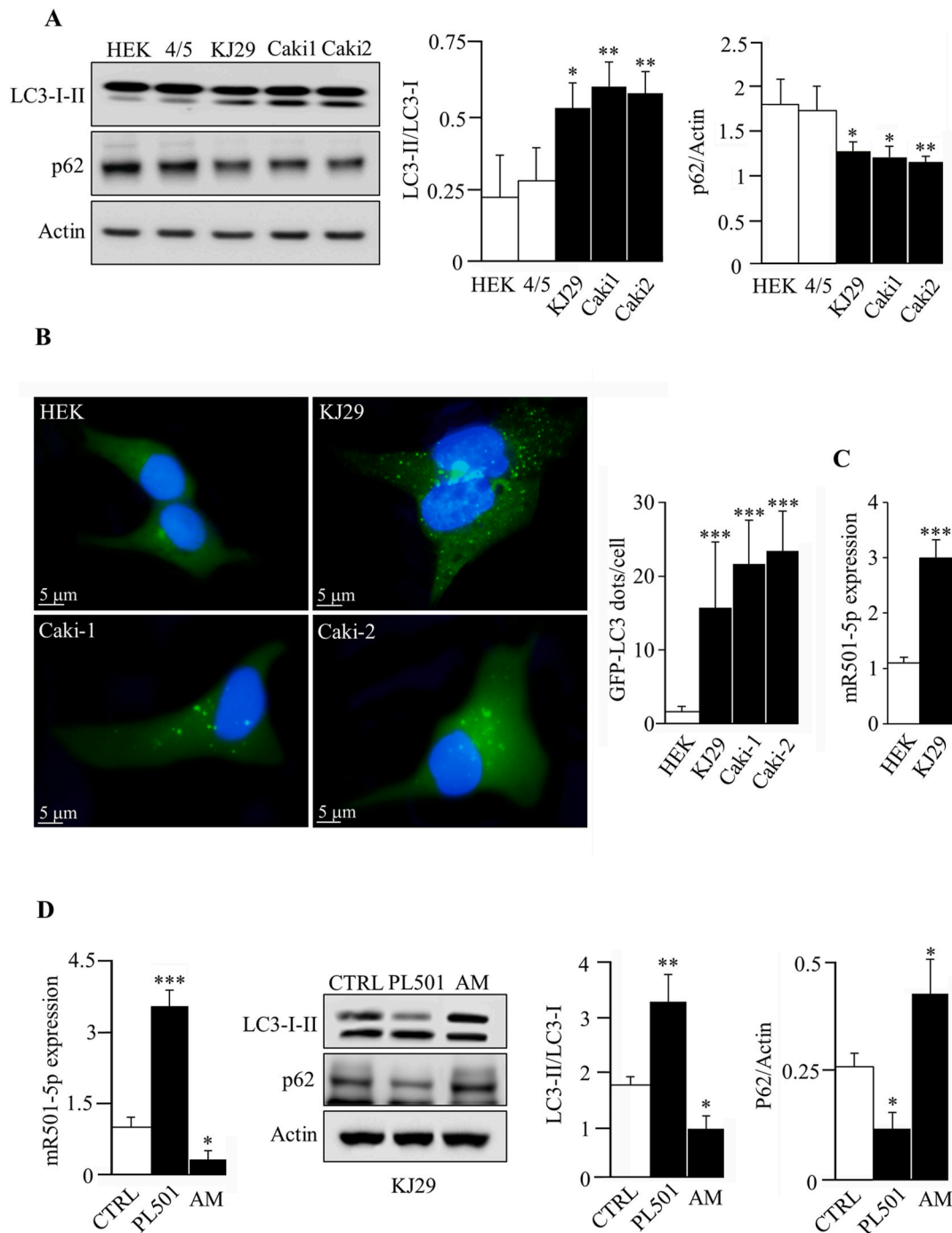


Fig. 1. Analysis of autophagy in control and cancer cells as well as in KJ29 tumor cells expressing different levels of miR501-5p. (A) Autophagy was analyzed by Western blotting using anti-LC3 and anti-p62/SQSTM1 antibodies in HEK293 and 4/5 control kidney cells as well as in KJ29, Caki-1 and Caki-2 tumor cells. The expression of LC3-II protein is higher, while the levels of p62/SQSTM1 are lower in cancer cells than in control cells (For LC3-II expression: KJ29 vs HEK293 $*p < 0.05$; Caki-1 and Caki-2 vs HEK293 $**p < 0.01$). For p62/SQSTM1 expression: KJ29 and Caki-1 vs HEK293 $*p < 0.05$; Caki-2 vs HEK293 $**p < 0.01$). (B) Autophagic vesicles were visualized by using a fluorescence microscope at $40\times$ magnification in HEK293, KJ29, Caki-1 and Caki-2 cells transfected with a recombinant plasmid expressing LC3 protein linked to GFP. Nuclei were stained with Dapi. Images were acquired by a CCD camera and processed by ImageJ software. KJ29, Caki-1 and Caki-2 tumor cells show more cytoplasmic dots than HEK293 control cells ($***p < 0.001$). (C) The analysis of miR501-5p expression by Real Time RT-PCR shows that KJ29 cells express higher levels of this miR than HEK293 cells ($***p < 0.001$). (D) The transfection of KJ29 cells with a plasmid that express miR501-5p sequences (PL501) increases the expression of this miR ($***p < 0.001$), enhances LC3-II levels ($**p < 0.01$) and reduces p62/SQSTM1 protein content ($*p < 0.05$) compared with cells transfected with an irrelevant plasmid (CTRL). Conversely, the treatment with antagonomiR sequences (AM) reduces miR501-5p expression, decreases the levels of LC3-II and increases those of p62/SQSTM1 ($*p < 0.05$). Data, expressed as mean \pm standard deviation, were obtained from three independent experiments. Statistical analysis was calculated by unpaired *t*-test for the section C, while for the other sections was evaluated by Anova test.

vector not only enhanced the expression of miR501-5p, but also increased the levels of LC3-II as well as reduced those of p62/SQSTM1 (Fig. 1D). Conversely, the treatment with AM sequences that reduced the levels of this miR reverted the expression of these autophagic markers (Fig. 1D). Consistently, the transfection of both HEK293 and KJ29 cells with either PL501 plasmid or AM enhanced and reduced the number of autophagosomes, respectively (Fig. 2A and B) confirming that the microRNA501-5p regulates autophagy in kidney cells. Notably, the accumulation of autophagosomes may be representative of activation of autophagic process, as well as a blockage of downstream steps of this pathway. In this latter case, autophagosomes accumulate due to an inefficient fusion or decreased lysosomal degradation. Different methods are used to verify the dynamic of LC3 turnover. Among them, the employment of a tandem fluorescent construct expressing the LC3 protein, linked to a green fluorescent protein and a red marked cherry (mCherry-eGFP-LC3) is the most used. When the autophagosome forms, both mCherry and GFP are present in the autophagic vesicle, which is yellow stained. Upon fusion with lysosome, the GFP signal disappears, due to its degradation by acid lysosomal proteases. Overall, a dynamic switch from yellow to red is representative of a functional LC3 turnover [20]. The presence of red dots in both HEK293 (Fig. 3A and C) and KJ29 cells (Fig. 3B and D) co-transfected with either PL501 or CTRL plasmid and mCherry-eGFP-LC3 vector were detected, indicating the presence of autophagolysosomes. The fusion of autophagosomes and lysosomes in autophagolysosomes suggests that the autophagic system is undamaged in both normal and tumor cells, and the overexpression of miR501-5p that positively modulates autophagy does not impair the autophagic flux.

3.2. MicroRNA501-5p increases mTOR independent autophagy through the activation of AMP kinase in a mechanism involving mitochondrial activity

We have previously reported that the upregulation of miR501-5p

increases the activity of mTOR kinase, an inhibitor of canonical autophagy [6]. Despite this, the overexpression of this miR caused a significant increase of autophagy (Figs. 1D and 2). To explain this apparent discrepancy, we have investigated mTOR-independent autophagy, inhibiting mTOR and analyzing the activity of AMP kinase, the main positive autophagy regulator [21]. As expected, the transfection of KJ29 cells with the PL501 plasmid enhanced both mTOR phosphorylation and LC3-II protein expression (Fig. 4A). Moreover, the treatment with rapamycin dramatically reduced mTOR phosphorylation in both KJ29 cells transfected either with PL501 or CTRL plasmid compared with untreated cells (Fig. 4A). However, rapamycin administration enhanced the expression of LC3-II only in cells transfected with the CTRL vector, but not in same cells transfected with the PL501 plasmid, where the levels of LC3-II remained unchanged (Fig. 4A on the right). These observations indicate that the activation of autophagy by miR501-5p upregulation is mTOR-independent. In fact, the phosphorylation of AMPK was found higher in KJ29 cells transfected with different amounts of PL501 plasmid than in those transfected with the CTRL vector (Fig. 4B), confirming that the overexpression of miR501-5p induced AMPK-dependent autophagy. Consistently, the inhibition of AMP kinase in KJ29 CTRL and PL501 transfected cells by treatment with compound C significantly reduced AMPK phosphorylation and LC3II expression (Fig. 4C). Moreover, the phosphorylation of the mammalian autophagy-initiating kinase (ULK1Ser317) that is directly phosphorylated by AMPK is enhanced in KJ29 cells transfected with the PL501 plasmid (Fig. 4D). The activation of AMP kinase may occur by mitochondrial dysfunction caused by the reduction of Ca^{2+} transfer to mitochondria, which is regulated by the mitochondrial calcium uniporter (MCU). The decreased mitochondrial activity leads to the inhibition of mTOR kinase promoting the AMPK-dependent pathway of autophagy [22]. Interestingly, the bioinformatic analysis revealed that the 3' UTR of MCU mRNA contains three seeding regions for the miR501-5p (Fig. 5A), therefore the increased expression of this miR should reduce MCU translation. Actually, the transfection of KJ29 cells

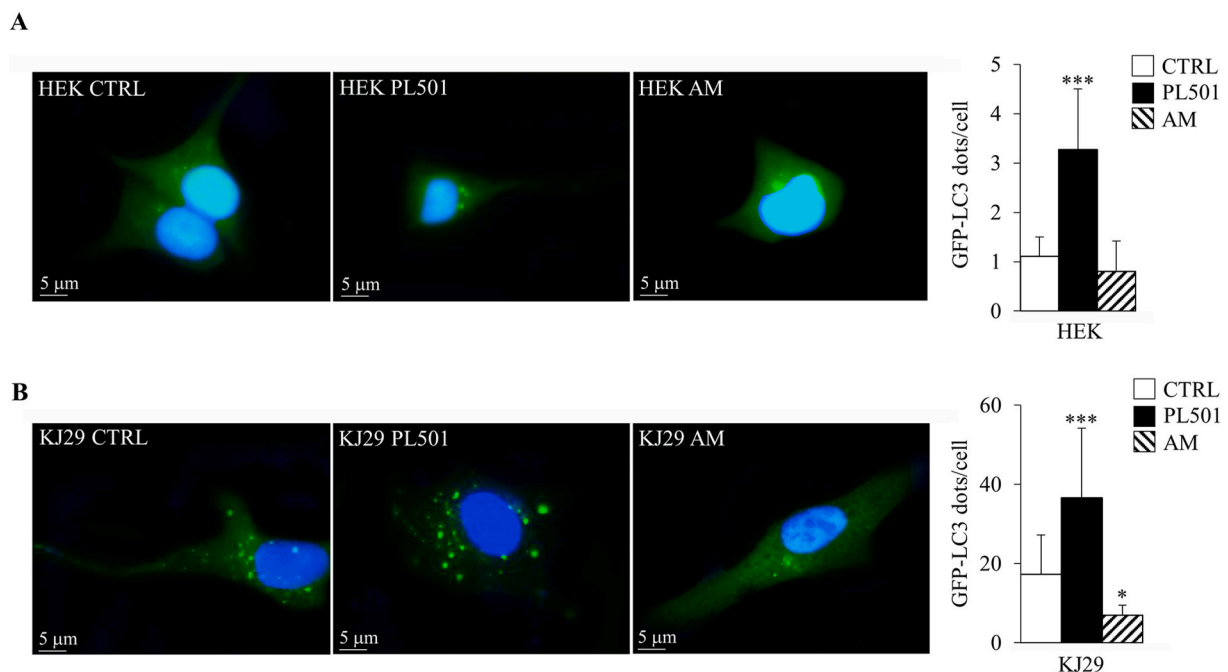


Fig. 2. Study of autophagy in HEK293 control and KJ29 tumor cells expressing miR501-5p exogenous sequences. HEK293 (A) and KJ29 (B) cells were transfected with either PL501 or CTRL vector as well as with antagomiR sequences (AM), mixed with a construct expressing the protein LC3 linked to GFP. Next, cells were analyzed by using a fluorescence microscope equipped with a CCD camera at 40× magnification. Nuclei were stained with dapi and images were processed by ImageJ program. The increased expression of miR501-5p enhances the formation of autophagic vesicles (green dots) in both HEK293 and KJ29 cells compared with control cells (** $p < 0.001$). The treatment with antagomiR causes a significant reduction of autophagosomes in KJ29 tumor cells (* $p < 0.05$). Data, expressed as mean \pm standard deviation, were calculated from three different experiments. Statistical significance was calculated by Anova test.

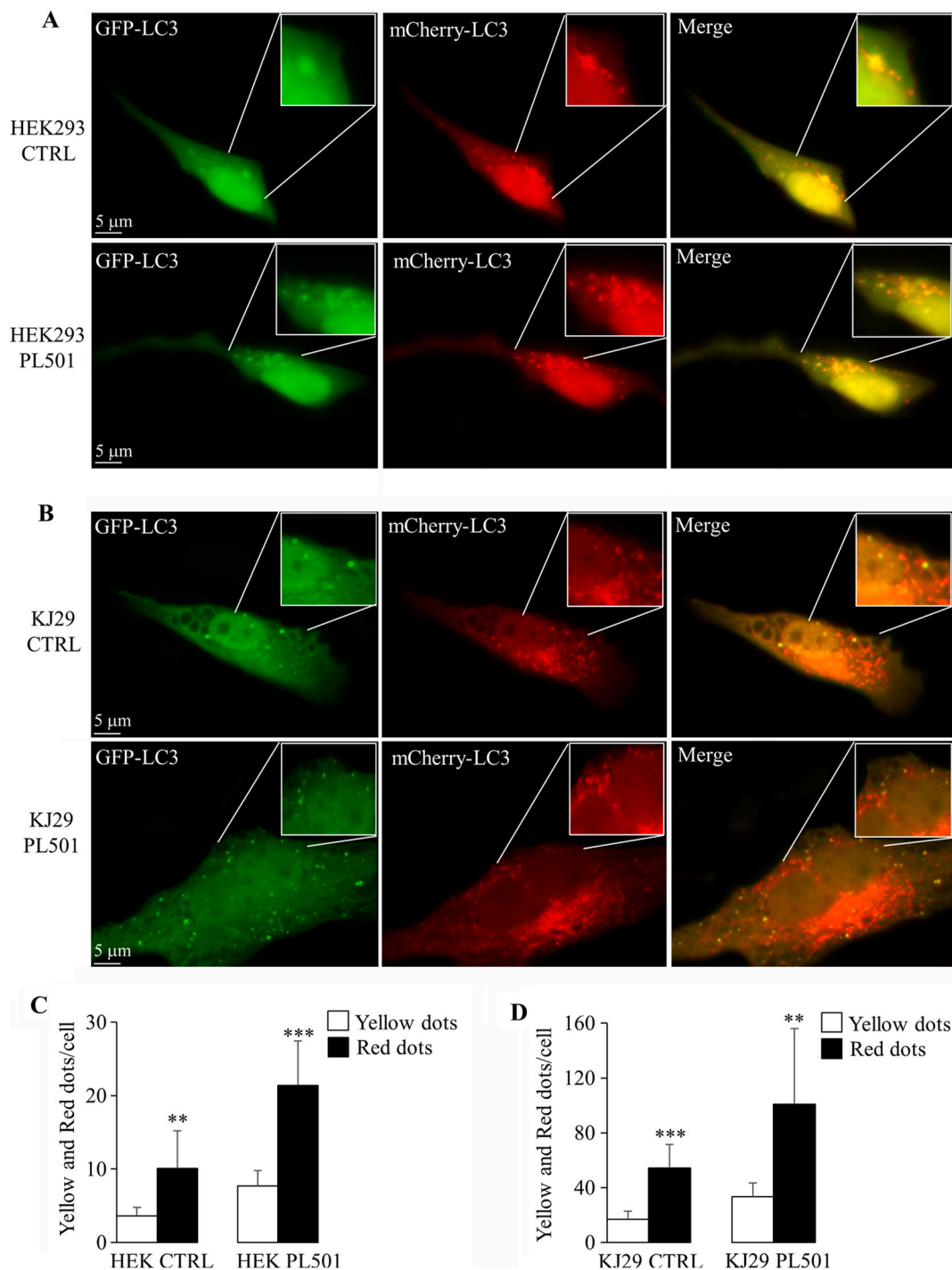


Fig. 3. Analysis of autophagic flux by using double tag LC3 protein in HEK293 and KJ29 cells transfected with the PL501 plasmid. HEK293 (A) and KJ29 (B) cells, seeded on 24 mm coverslips and cultured in six-well plates overnight, were co-transfected with either PL501 or CTRL plasmid in combination with mCherry-eGFP-LC3 vector for 24 h. Next, cells were washed, fixed and visualized through a fluorescence microscope at 40 \times magnification. Images, collected through a CCD camera, were processed by ImageJ software. The upregulation of miR501-5p does not block the autophagic flux as shown by the presence of red dots (acidic vesicles). As expected, the number of red dots is greater than yellow ones in both HEK293 (C) and KJ29 (D) cells (red vs yellow dots: ** p < 0.01 in HEK CTRL and KJ29 PL501 cells; *** p < 0.001 in HEK PL501 and KJ29 CTRL). Data, expressed as mean \pm standard deviation, were obtained from three independent experiments. Statistical analysis was performed by unpaired t -test.

with the PL501 plasmid caused a strong decrease of MCU protein levels compared with same cells transfected with the CTRL vector (Fig. 5B). Moreover, HEK293 cells co-transfected with this plasmid and a construct containing the 3' UTR of MCU mRNA inserted downstream of luciferase gene showed a marked reduction of luciferase activity (Fig. 5C). As expected, the reduced MCU protein synthesis due to miR501-5p

overexpression affected mitochondrial Ca^{2+} uptake causing a significant reduction of calcium levels into mitochondria after ATP stimulation (Fig. 5D). Consequently, the reduction of intra-mitochondrial calcium drops mitochondrial activity inducing a significant decrease of ATP synthesis detected by a luciferase system (Fig. 5E). Taken together, these findings indicates that miR501-5p is able to promote AMPK-dependent

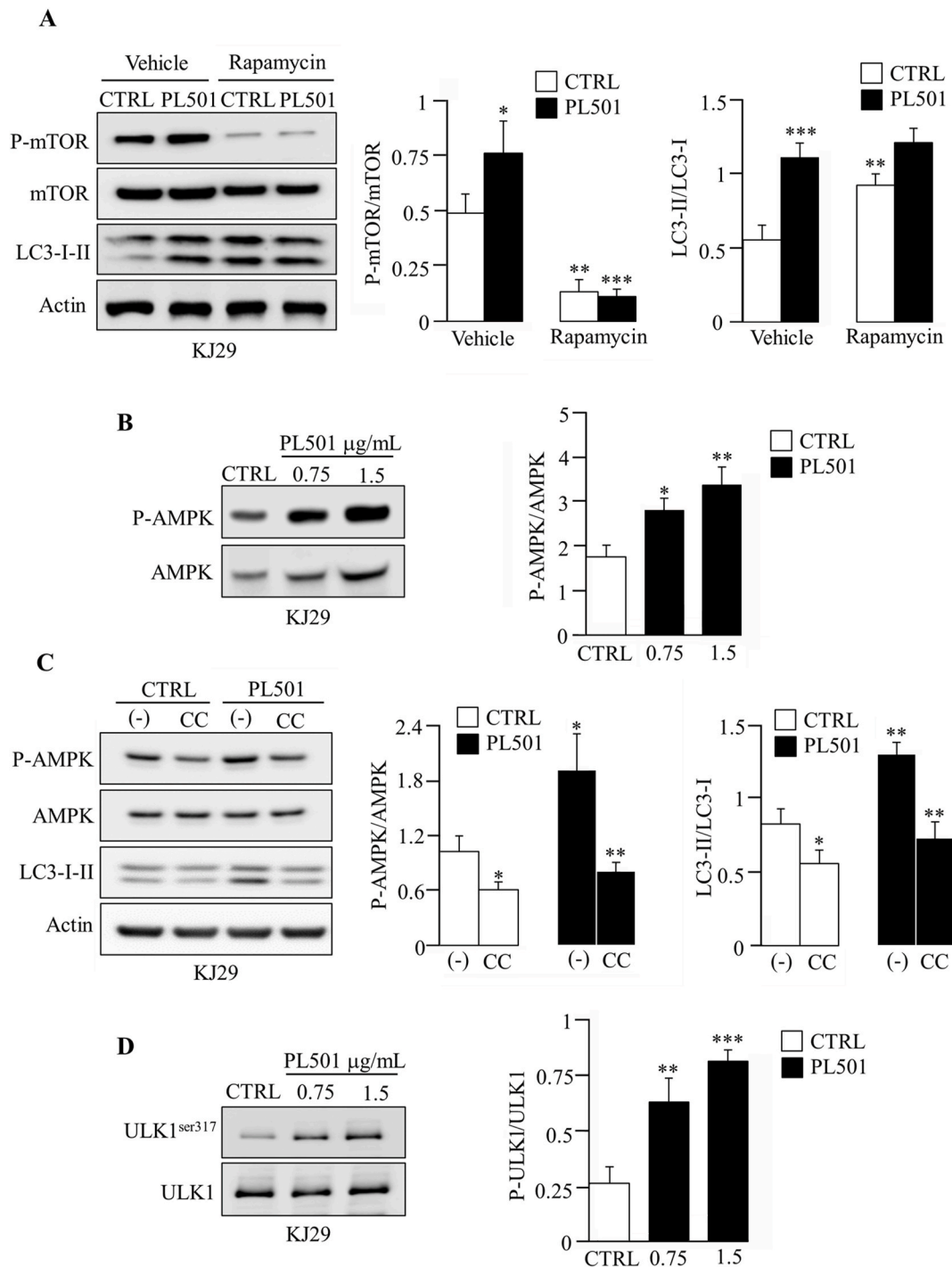


Fig. 4. Study of autophagy by AMPK activity and mTOR inhibition in KJ29 cells transfected with the PL501 plasmid. (A) The transfection of KJ29 cells with the PL501 plasmid enhances the phosphorylation of mTOR and the levels of LC3-II protein ($*p < 0.05$ and $***p < 0.001$, respectively). The treatment with rapamycin (500 nM) for 24 h dramatically reduces mTOR activity in KJ29 cells transfected with both CTRL and PL501 plasmids compared with cells treated with vehicle ($**p < 0.01$ and $***p < 0.001$, respectively). The inhibition of mTOR increases LC3-II protein levels in cells transfected with the CTRL plasmid ($**p < 0.01$), but not in those transfected with the PL501 vector. (B) The transfection of KJ29 cells with different amounts of PL501 plasmid increases the phosphorylation of AMPK as compared to cells transfected with the CTRL vector ($*p < 0.05$ and $**p < 0.01$). (C) KJ29 cells transfected with CTRL or PL501 plasmid (1.5 $\mu\text{g}/\text{mL}$) were treated with 5 μM of compound C (CC) an inhibitor of AMPK for 24 h. The transfection with PL501 plasmid increases the phosphorylation of AMPK and the expression of LC3II compared with control cells ($*p < 0.05$ for AMPK and $**p < 0.01$ for LC3II). The treatment with compound C reduces AMPK phosphorylation and LC3II expression in both CTRL and PL501 transfected cells as compared to untreated cells (CTRL + CC vs CTRL: $*p < 0.05$; PL501 + CC vs PL501: $**p < 0.01$). (D) The transfection of KJ29 cells with increased doses of PL501 plasmid enhances the phosphorylation of ULK1Ser317 compared with CTRL cells ($**p < 0.01$ and $***p < 0.001$). Data, expressed as mean \pm standard deviation, were calculated from three different experiments. Statistical analysis was performed by unpaired *t*-test for sections A and C, while for sections B and D was calculated by Anova test.

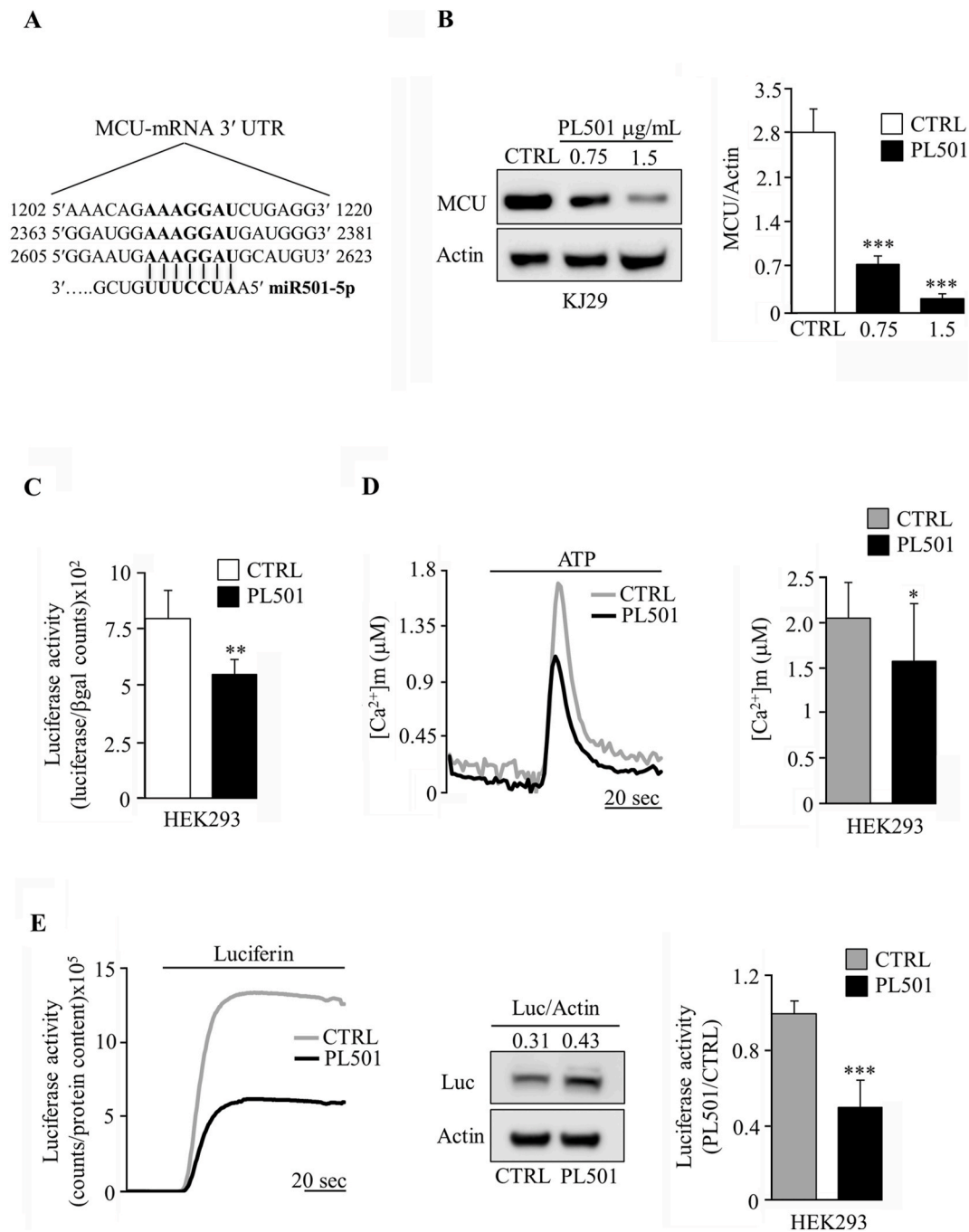


Fig. 5. Analysis of MCU expression, mitochondrial calcium uptake and ATP generation in kidney cells upregulated for miR501-5p. (A) Three putative target sites for miR501-5p localized at the 3' UTR of MCU mRNA are indicated. Bioinformatic analysis was performed by using TargetScan software and the position of miR501-5p sites on MCU cDNA (GenBank accession number: NM_138357.2) are shown in supplementary file 1. (B) The transfection of KJ29 cells with different amounts of PL501 plasmid that express miR501-5p sequences reduces MCU protein levels compared with cells transfected with the CTRL vector ($***p < 0.001$). (C) The transfection of HEK293 cells with the PL501 plasmid in combination with a vector containing the 3' UTR of MCU mRNA fused with the Luciferase gene reduces the activity of Luciferase enzyme compared with CTRL cells ($**p < 0.01$). (D) The analysis of mitochondrial Ca²⁺ influx was performed by aequorin system in HEK293 cells transfected with either PL501 or CTRL plasmid in combination with the mtAEQ vector expressing the photoprotein aequorin targeted to mitochondria. The increased expression of miR501-5p causes the decrease of mitochondrial Ca²⁺ uptake after stimulation with 100 μ M ATP as compared to cells transfected with the CTRL vector ($*p < 0.05$). (E) ATP generation was measured by a luminometer in HEK293 cells transfected as described above by using a vector expressing the luciferase gene. Luciferase protein levels, detected by Western blotting, were used for sample normalization. The reduction of luciferase activity reveals a lower ATP synthesis in HEK293 transfected with the plasmid PL501 than in those transfected with the CTRL vector ($***p < 0.001$). Experiments shown in sections C, D and E were performed in HEK293 cells because they are easier to transfect especially using a combination of different plasmids. Data, expressed as mean \pm standard deviation, were obtained from three different experiments. Statistical significance was performed by Anova test for the section B, while for the other sections was calculated by unpaired *t*-test.

autophagy by mitochondrial dysfunction through a mechanism involving the downregulation of MCU channel.

3.3. The activation of autophagy by miR501-5p overexpression induces the degradation of p53 in kidney cancer cells

We described that the overexpression of miR501-5p induced the ubiquitination of p53 by the increase of mTOR/MDM2 pathway leading to its inactivation via proteasomal machinery in kidney cancer cells [6]. Nevertheless, the activation of AMPK-dependent autophagy by the upregulation of miR501-5p could induce the degradation of p53 protein also through this biological process. To test this hypothesis, KJ29 and Caki-2 kidney cancer cells were co-transfected either with PL501 or CTRL plasmid and a construct expressing wild type p53 linked to GFP. Next, cells were treated with an anti-LC3 antibody conjugated with rhodamine in order to recognize autophagic structures. As shown in Fig. 6 and Supplementary Fig. 1, p53-GFP protein (green staining) is

confined not only to the cytoplasm, but also in dot structures especially in cells transfected with the PL501 plasmid, suggesting that this tumor suppressor could be trapped inside autophagosomes. Actually, the protein p53, included in most of these vesicles, co-localizes with the autophagic marker LC3 (yellow dots), confirming that part of this onco-suppressor is seized and degraded by the autophagic machinery.

3.4. Autophagy inhibition restores p53 expression leading to the reduction of cell growth and migration

Because p53 may be caught and removed by autophagosomes, the inhibition of autophagy should restore the levels of this tumor suppressor. The inhibition of autophagy was performed by cell transduction with recombinant lentiviruses expressing specific shRNAs (shATG7) for the silencing of *ATG7* gene. As control, cells were infected with lentivirus particles containing the wild type vector (pLKO). As expected, the infection of KJ29 and Caki-2 cells with shATG7 lentiviruses significantly

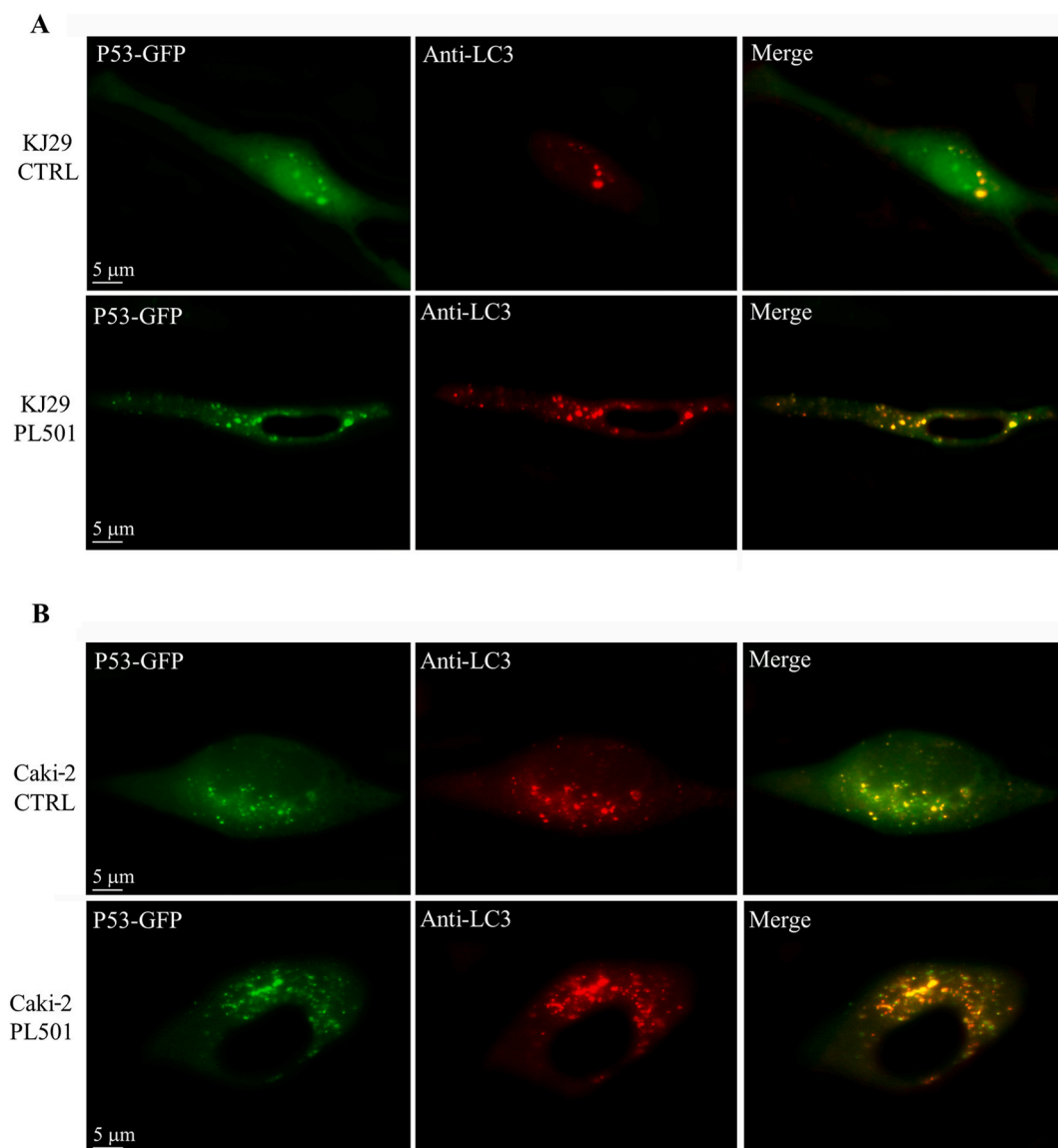


Fig. 6. Analysis of p53-GFP subcellular localization by fluorescence microscopy in cancer cells expressing miR501-5p exogenous sequences. KJ29 (A) and Caki-2 (B) cells, seeded on 24 mm coverslips and cultured in six-well plates overnight, were co-transfected with either PL501 or CTRL plasmid and a recombinant vector expressing wild type p53 linked to GFP for 24 h. Next, cells were fixed, permeabilized and treated, first, with an anti-LC3 primary antibody and then with a secondary antibody conjugated with rhodamine. Finally, cells were analyzed by a fluorescent microscope at 40 \times magnification and images were processed by using ImageJ software. Wild type p53 protein fused to GFP co-localizes with the autophagic marker LC3 in cytoplasmic vesicles (yellow dots). The transfection with the PL501 plasmid enhances the number of autophagosomes containing the p53 protein in both KJ29 and Caki-2 cells.

reduced ATG7 protein expression compared with same cells transduced with the control virus (Fig. 7A). Moreover, the silencing of *ATG7* gene caused the reduction of LC3-II expression indicating the occurred autophagy inhibition (Fig. 7A). The reduction of autophagy enhanced the levels of p53 protein in both KJ29 and Caki-2 cells (Fig. 7B), confirming that this process may be used by cancer cell to remove p53. Consistently, a significant increase of p21 protein expression that is positively modulated by p53 and a strong decrease of cell proliferation in both cell lines transduced with shATG7 lentivirus it has been observed (Fig. 7B and C).

It is known that *TP53* loss of function induces epithelial mesenchymal transition (EMT) promoting tumor progression in gastric cancer [23]. Since autophagy modulates the expression of p53 protein, it could affect EMT also in kidney cancer cells. In order to test this assumption, we have inhibited autophagy by cell transduction with shATG7 lentivirus and analyzed EMT evaluating the levels of E-Cadherin and Vimentin that are specific epithelial and mesenchymal markers, respectively. The inhibition of autophagy increased the content of E-Cadherin and reduced the levels of Vimentin in both KJ29 and Caki-2 cells (Fig. 8A). However, the silencing of *TP53* significantly reduces E-Cadherin expression but does not modify the levels of Vimentin

(Fig. 8B). Moreover, a slower cell migration in both KJ29 and Caki-2 cell lines silenced for *ATG7* gene than in control cells was detected (Fig. 8C and D). These findings indicate that the inhibition of autophagy in kidney cancer cells leads to the reduction of cell growth, migration and EMT in a mechanism involving p53 and, likely, other signaling pathways.

4. Discussion

Autophagy in cancer is not yet well defined, since it seems to work differently depending on cellular context. In the early stage of disease, autophagy may act as a mechanism of tumor suppression preventing cell proliferation and inflammation [24]. However, in disease recurrence or metastasis this process could promote cancer progression and therapy resistance [24,25]. Here, we report that different kidney tumor cell lines show increased levels of autophagy compared with control kidney cells, therefore it could be associated with cancer progression. Previously, we have described that miR501-5p which is upregulated in ccRCC cells as well as in tumor tissues of patients with advanced disease, seems to correlate with poor prognosis [6]. We postulate that the upregulation of this miR may activate autophagy in kidney cancer cells. Actually, the

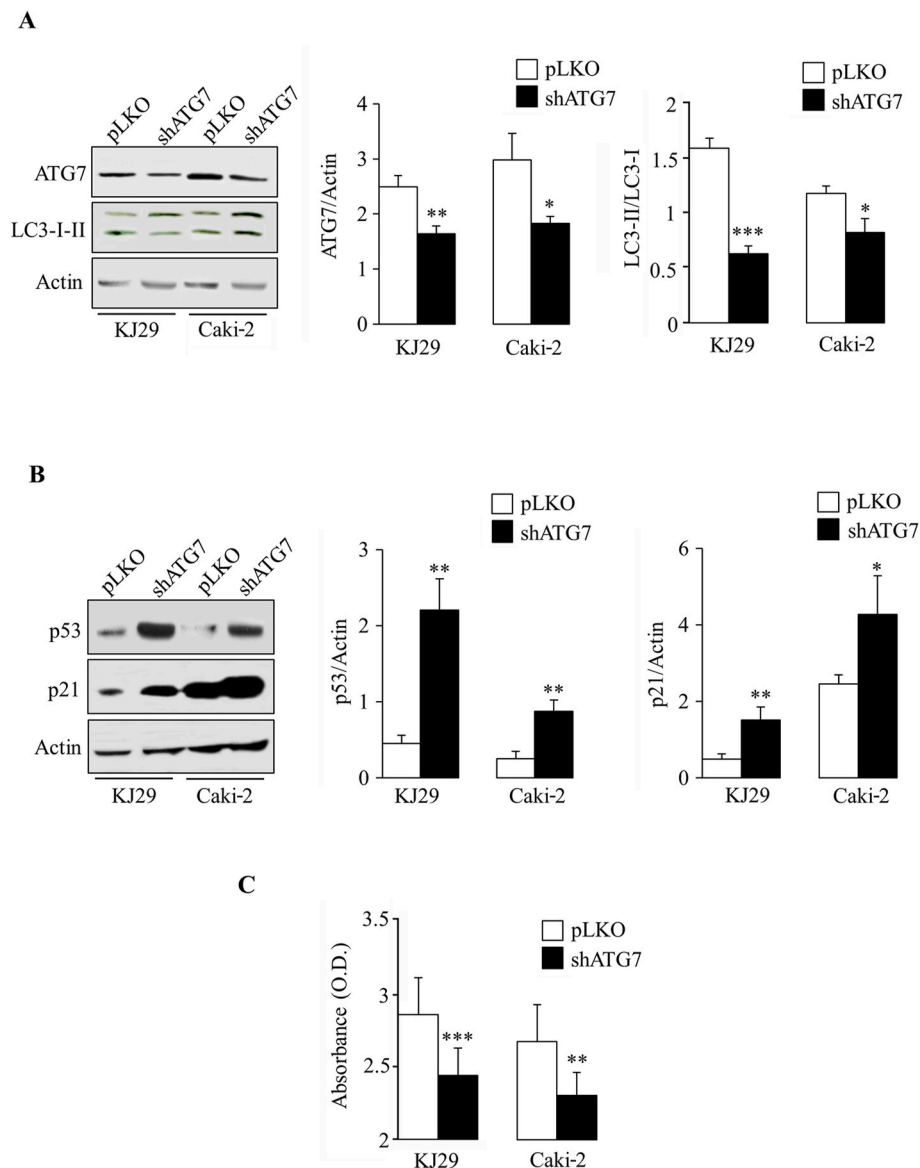


Fig. 7. Study of p53 and p21 protein expression and cell proliferation after the inhibition of autophagy in kidney cancer cells. (A) KJ29 and Caki-2 cells were transduced with recombinant lentiviruses (shATG7) able to suppress the *ATG7* gene or with the control virus (pLKO). The infection of KJ29 and Caki-2 with shATG7 causes the reduction of ATG7 protein expression in both cells lines compared with pLKO transduced cells (** $p < 0.01$ for KJ29 and * $p < 0.05$ for Caki-2). Consistently, the silencing of *ATG7* gene reduces the levels of LC3-II protein (** $p < 0.001$ for KJ29 and * $p < 0.05$ for Caki-2). (B) The inhibition of autophagy by transduction of KJ29 and Caki-2 cells with shATG7 lentiviruses increases both p53 and p21 protein expression compared with pLKO transduced cells (** $p < 0.01$ for p53; ** $p < 0.01$ and * $p < 0.05$ for p21). (C) The silencing of *ATG7* gene reduces cell proliferation in both KJ29 and Caki-2 cells compared with control ones (** $p < 0.001$ for KJ29 and ** $p < 0.01$ for Caki-2). Data, expressed as mean \pm standard deviation, were obtained from three independent experiments for sections A and B, while for the section C data were calculated from four experiments. Statistical significance was performed by using unpaired *t*-test.

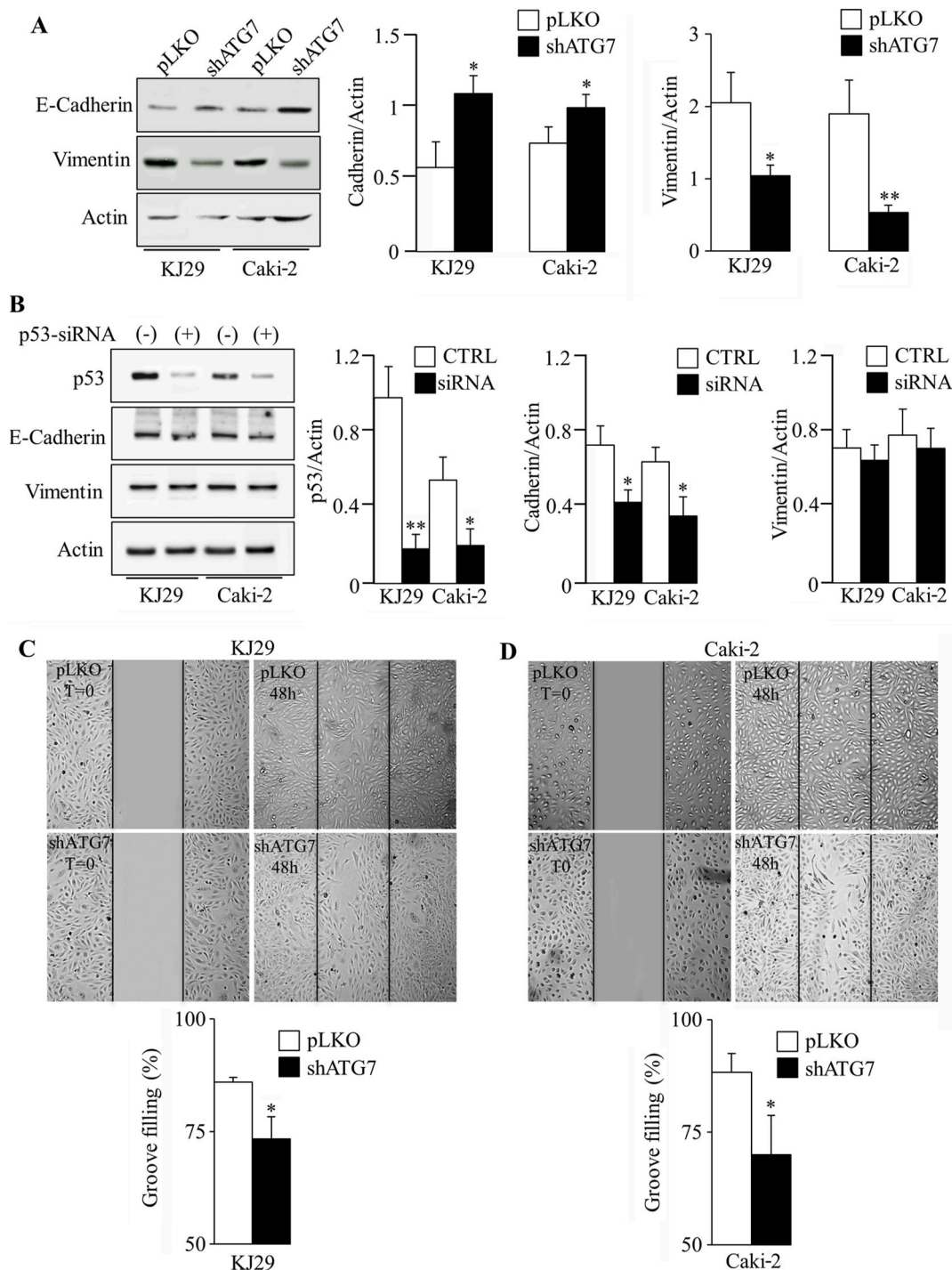


Fig. 8. Evaluation of cell migration and epithelial mesenchymal transition (EMT) by E-Cadherin and Vimentin expression in kidney cancer cells silenced for *ATG7* gene. (A) The inhibition of autophagy in KJ29 and Caki-2 cells transduced with shATG7 lentiviruses increases the levels of E-Cadherin and reduces the expression of Vimentin compared with cells infected with pLKO (* $p < 0.05$ for E-Cadherin; * $p < 0.05$ and ** $p < 0.01$ for Vimentin). (B) The silencing of *TP53* reduces both p53 and E-Cadherin protein levels but not changes those of Vimentin in KJ29 and Caki-2 cells (** $p < 0.01$ and * $p < 0.05$ for p53 in KJ29 and Caki-2, respectively; * $p < 0.05$ for E-Cadherin in both cell types). The inhibition of autophagy by ATG7 silencing in KJ29 cells (C) and Caki-2 cells (D) causes a significant reduction of cell migration in comparison with pLKO transduced cells (* $p < 0.05$). Images were acquired by a contrast phase microscope equipped with a CCD camera at 4 \times magnification. The percentage of groove filling was calculated by ImageJ software. Data expressed as mean \pm standard deviation were obtained from three different experiments. Statistical significance was calculated by unpaired *t*-test.

exogenous overexpression of miR501-5p in our renal cellular models promotes autophagy confirming that this miR may modulate this biological process. However, the miR501-5p also increases the activity of mTOR kinase and thus it should inhibit the autophagic machinery. Therefore, we speculate that the upregulation of this miR may stimulate

the mTOR-independent autophagy in kidney cancer cells. Accordingly, different tumors take advantage of this type of autophagy in response to cellular stress or starvation, so that the cell undergoes a form of self-eating to use as source of energy [26]. As postulated, the increased autophagy observed in KJ29 tumor cells overexpressing the miR501-5p

is mTOR-independent, because it is not induced by the inhibition of this protein kinase. The triggering of autophagy could be supported by the induction of AMP kinase that is activated in case of low energy availability [27]. In fact, we have observed a strong increase in AMPK phosphorylation in KJ29 cells overexpressing miR501-5p. Consistently, the inhibition of AMPK by cell treatment with compound C strongly reduces both AMPK phosphorylation and LC3II expression. The activation of AMPK by the overexpression of miR501-5p leads to the phosphorylation of ULK1^{Ser317}, which stimulates mTOR-independent autophagy [28,29]. Taken together, these findings indicate that autophagy induction by miR501-5p overexpression is driven through AMPK-ULK1 pathway in kidney cancer cells. AMPK, a highly conserved sensor of intracellular adenosine nucleotide levels, is a sensor of the energy status of the cell, and is activated by ATP decreasing [27]. AMPK, induced by mitochondrial dysfunction, phosphorylates BECN1 initiating autophagy through mTOR-independent mechanisms [27]. The reduction of mitochondrial activity may occur by the impairment of Ca²⁺ influx into the mitochondrion that may compromise cell bioenergetics leading to metabolic stress and activating the autophagic pathway [22]. The Ca²⁺ uptake through mitochondria is regulated by the mitochondrial calcium uniporter (MCU) and is used by the dehydrogenases of TCA cycle for ATP generation [30,31]. The upregulation of miR501-5p is able to inhibit MCU protein synthesis by targeting the 3'UTR of MCU mRNA. Consequently, the decrease of MCU channel protein induces a significant reduction of mitochondrial Ca²⁺ levels after ATP stimulation, suggesting that miR501-5p is able to modulate mitochondrial Ca²⁺ uptake. As expected, the decrease of Ca²⁺ influx into the mitochondria causes a robust lowering of mitochondrial activity resulting in reduced ATP generation.

Taken together, our observations show that miR501-5p upregulation causes the reduction of both mitochondrial calcium influx and energy production by the downregulation of MCU protein levels leading to the activation of AMPK that in turn promotes mTOR-independent autophagy.

Interestingly, autophagy may be used by tumor cell to degrade ubiquitinated proteins [32]. Our previous observations show that the tumor suppressor p53 is ubiquitinated through the activation of mTOR/MDM2 pathway in renal cancer cells [6]. Thus, part of p53 protein could be degraded by the autophagic system. Actually, the exogenous expression of wild type p53 co-localizes with autophagosomal structures, in particular, in tumor cells overexpressing miR501-5p sequences, suggesting that the autophagic machinery is used by kidney cancer cells to remove this oncosuppressor. Consistently, the inhibition of autophagy causes a dramatic increase of p53 levels confirming that this process contributes to p53 inactivation. Furthermore, the reduction of autophagy leads to the induction of the cell cycle inhibitor p21 and the inhibition of cell proliferation likely through the increased expression of p53. The tumor suppressor p53 may also regulate EMT, in fact, the loss of p53 induces EMT in gastric epithelial cells [23]. In addition, p53 inhibits the RAS-mediated EMT and EMT-associated stemness of human mammary epithelial cells increasing the expression of E-Cadherin and β -Catenin [33]. Accordingly, the inhibition of autophagy that restores p53 expression leads to the reduction of both cell migration and EMT through the upregulation of E-Cadherin and the downregulation of Vimentin. However, the silencing of *TP53* causes the reduction of E-Cadherin but not affects the expression of Vimentin suggesting that the decrease of autophagy reduces EMT also through the involvement of other factors. Moreover, the link between autophagy and EMT is still unclear because some studies show that the inhibition of autophagy promotes EMT in different cancer types [33], while other observations report that the silencing of *ATG3* and *ATG7* genes suppresses EMT in hepatocellular carcinoma cells [33]. Our findings support data involving autophagy in disease progression promoting cell growth, expansion and EMT also by p53/p21 contribution. Furthermore, it is well known that in different tumors including kidney cancer the p53/p21 pathway has been found impaired [34]. Thus, the reactivation of p53 could represent an

important option for the treatment of advanced kidney carcinoma. In this regard, interventions aimed at restoration of p53 expression by using MDM2-proteasome inhibitors showed encouraging results in pre-clinical models and have been approved for clinical trials in different tumors [35]. However, the role of p53 in kidney cancer remains unclear and is still debated, because the overexpression of this tumor suppressor may be associated with poor prognosis [36]. This apparent paradox could be due to the acquisition of sequential mutations of *TP53* gene in cancer cells during tumorigenesis, which may generate oncogenic peptides, contributing to cancer development and progression [37]. Moreover, p53 dysfunction may also activate autophagy, because the deletion, depletion or inhibition of *TP53* induces autophagy in human and mouse cells [38]. Consistently, mutations of p53 can disrupt the ability of this tumor suppressor to downregulate autophagy promoting tumor aggressiveness in colorectal cancer [39]. Based on these observations, the design of therapies solely addressed to the increase of p53 levels, such as the targeting of MDM2-proteasome proteins, should be carefully evaluated in order to prevent the synthesis of p53-mutated peptides, which may activate both oncogenic signals and autophagy.

In summary, we report that kidney cancer cells activate mTOR-independent autophagy leading to p53 inactivation in a mechanism involving the upregulation of miR501-5p, the downregulation of MCU, the drop of energy availability that consequently sustain the autophagic status through the AMPK-ULK1 axis.

The inhibition of autophagy by *ATG7* gene silencing restores p53/p21 axis, reduces both cell growth and migration and negatively regulates EMT through the upregulation of E-Cadherin and the downregulation of Vimentin.

Findings obtained by our cellular models for kidney cancer support the hypothesis that autophagy may provide for the recovery of energy metabolites needed for cancer cell growth and progression in renal carcinoma, as observed by some authors in kidney cancer and other tumors [24,25,40,41].

Finally, the targeting of autophagic proteins could be a promising option for the treatment of metastatic kidney carcinoma, since the inhibition of autophagy may restore p53 function and, at the same time, subtract energy resources crucial for cancer cell survival.

Declaration of competing interest

None.

CRediT authorship contribution statement

Simone Patergnani: Validation, Investigation, Conceptualization, Project administration, Funding acquisition. **Sonia Guzzo:** Investigation. **Alessandra Mangolini:** Investigation, Funding acquisition. **Lucio dell'Atti:** Resources, Visualization. **Paolo Pinton:** Conceptualization, Writing - review & editing, Project administration, Funding acquisition. **Gianluca Aguiari:** Conceptualization, Formal analysis, Data curation, Writing - original draft, Supervision, Project administration, Funding acquisition.

Acknowledgements

We thank Prof. A. D. Schimmer (Princess Margaret Hospital, Toronto, Canada) for providing p53-GFP vector, Prof. Guido Kroemer (Centre de Recherche des Cordeliers, Paris, France) for LC3-GFP construct and Prof. Paola Rusmini (University of Milan, Italy) for mCherry-eGFP-LC3 recombinant plasmid. This work was supported by the following funds: from G.A., University of Ferrara local Funds; from A.M., Ricerca Finalizzata 2011–2012 Grant: GR-2011-02346964; from P.P., AIRC (IG-18624), Telethon (GGP11139B) and University of Ferrara local funds; from S.P., Fondazione Umberto Veronesi.

Appendix A. Supplementary data

Supplementary data to this article can be found online at <https://doi.org/10.1016/j.yexcr.2020.112190>.

References

- [1] U. Capitanio, K. Bensalah, A. Bex, S.A. Boorjian, F. Bray, J. Coleman, J.L. Gore, M. Sun, C. Wood, P. Russo, Epidemiology of renal cell carcinoma, *Eur. Urol.* 75 (2019) 74–84.
- [2] J. Casuscelli, Y.A. Vano, W.H. Fridman, J.J. Hsieh, Molecular classification of renal cell carcinoma and its implication in future clinical practice, *Kidney cancer 1* (2017) 3–13.
- [3] C. D'Avella, P. Abbosh, S.K. Pal, D.M. Geynisman, Mutations in Renal Cell Carcinoma, *Urologic oncology*, 2018.
- [4] N. Cancer, Genome Atlas Research, Comprehensive molecular characterization of clear cell renal cell carcinoma, *Nature* 499 (2013) 43–49.
- [5] A.P. Noon, N. Vlatkovic, R. Polanski, M. Maguire, H. Shawki, K. Parsons, M. T. Boyd, p53 and MDM2 in renal cell carcinoma: biomarkers for disease progression and future therapeutic targets? *Cancer* 116 (2010) 780–790.
- [6] A. Mangolini, A. Bonon, S. Volinia, G. Lanza, R. Gambari, P. Pinton, G.R. Russo, L. Del Senno, L. Dell'Atti, G. Aguiari, Differential expression of microRNA501-5p affects the aggressiveness of clear cell renal carcinoma, *FEBS open bio* 4 (2014) 952–965.
- [7] L. de Stephanis, A. Mangolini, M. Servello, P.C. Harris, L. Dell'Atti, P. Pinton, G. Aguiari, MicroRNA501-5p induces p53 proteasome degradation through the activation of the mTOR/MDM2 pathway in ADPKD cells, *J. Cell. Physiol.* 233 (2018) 6911–6924.
- [8] V.D. Li, K.H. Li, J.T. Li, TP53 mutations as potential prognostic markers for specific cancers: analysis of data from the Cancer Genome Atlas and the International Agency for Research on Cancer TP53 Database, *J. Canc. Res. Clin. Oncol.* 145 (2019) 625–636.
- [9] M. Mrakovcic, L.F. Frohlich, p53-Mediated molecular control of autophagy in tumor cells, *Biomolecules* 8 (2018).
- [10] J.S. Carew, C.M. Espitia, W. Zhao, Y. Han, V. Visconte, J. Phillips, S.T. Nawrocki, Disruption of autophagic degradation with ROC-325 antagonizes renal cell carcinoma pathogenesis, clinical cancer research, *Off. J. Am. Assoc. Canc. Res.* 23 (2017) 2869–2879.
- [11] B. Greef, T. Eisen, Medical treatment of renal cancer: new horizons, *Br. J. Canc.* 115 (2016) 505–516.
- [12] S. Marchi, L. Lupini, S. Patergnani, A. Rimessi, S. Missiroli, M. Bonora, A. Bononi, F. Corra, C. Giorgi, E. De Marchi, F. Poletti, R. Gafa, G. Lanza, M. Negrini, R. Rizzuto, P. Pinton, Downregulation of the mitochondrial calcium uniporter by cancer-related miR-25, *Curr. Biol.* : CB 23 (2013) 58–63.
- [13] M. Loghman-Adham, S.M. Nauli, C.E. Soto, B. Kariuki, J. Zhou, Immortalized epithelial cells from human autosomal dominant polycystic kidney cysts, *Am. J. Physiol. Ren. Physiol.* 285 (2003) F397–F412.
- [14] C. Barletta, A. Bartolazzi, G. Cimino Reale, R. Gambari, C. Nastruzzi, R. Barbieri, L. Del Senno, A. Castagnoli, P.G. Natali, Cytogenetic, molecular and phenotypic characterization of the newly established renal carcinoma cell line KJ29. Evidence of translocations for chromosomes 1 and 3, *Anticancer Res.* 15 (1995) 2129–2136.
- [15] A. Bonon, A. Mangolini, P. Pinton, L. Del Senno, G. Aguiari, Berberine slows cell growth in autosomal dominant polycystic kidney disease cells, *Biochem. Biophys. Res. Commun.* 441 (2013) 668–674.
- [16] G. Aguiari, F. Bizzarri, A. Bonon, A. Mangolini, E. Magri, M. Pedriali, P. Querzoli, S. Somlo, P.C. Harris, L. Catizone, L. Del Senno, Polycystin-1 regulates amphiregulin expression through CREB and AP1 signalling: implications in ADPKD cell proliferation, *J. Mol. Med.* 90 (2012) 1267–1282.
- [17] M. Bonora, C. Giorgi, A. Bononi, S. Marchi, S. Patergnani, A. Rimessi, R. Rizzuto, P. Pinton, Subcellular calcium measurements in mammalian cells using jellyfish photoprotein aequorin-based probes, *Nat. Protoc.* 8 (2013) 2105–2118.
- [18] S. Patergnani, F. Baldassari, E. De Marchi, A. Karkucinska-Wieckowska, M. R. Wieckowski, P. Pinton, Methods to monitor and compare mitochondrial and glycolytic ATP production, *Methods Enzymol.* 542 (2014) 313–332.
- [19] A.G. Smith, K.F. Macleod, Autophagy, cancer stem cells and drug resistance, *J. Pathol.* 247 (2019) 708–718.
- [20] S. Patergnani, S. Marchi, A. Rimessi, M. Bonora, C. Giorgi, K.D. Mehta, P. Pinton, PRKCB/protein kinase C, beta and the mitochondrial axis as key regulators of autophagy, *Autophagy* 9 (2013) 1367–1385.
- [21] G. Rehman, A. Shehzad, A.L. Khan, M. Hamayun, Role of AMP-activated protein kinase in cancer therapy, *Arch. Pharmazie* 347 (2014) 457–468.
- [22] C. Cardenas, J.K. Foskett, Mitochondrial Ca(2+) signals in autophagy, *Cell Calcium* 52 (2012) 44–51.
- [23] J. Ohtsuka, H. Oshima, I. Ezawa, R. Abe, M. Oshima, R. Ohki, Functional loss of p53 cooperates with the in vivo microenvironment to promote malignant progression of gastric cancers, *Sci. Rep.* 8 (2018) 2291.
- [24] E. Bishop, T.D. Bradshaw, Autophagy modulation: a prudent approach in cancer treatment? *Canc. Chemother. Pharmacol.* 82 (2018) 913–922.
- [25] O. Mikhaylova, Y. Stratton, D. Hall, E. Kellner, B. Ehmer, A.F. Drew, C.A. Gallo, D. R. Plas, J. Biesiada, J. Meller, M.F. Czyzyk-Krzeska, VHL-regulated MiR-204 suppresses tumor growth through inhibition of LC3B-mediated autophagy in renal clear cell carcinoma, *Canc. Cell* 21 (2012) 532–546.
- [26] A.M. Hau, J.A. Greenwood, C.V. Lohr, J.D. Serrill, P.J. Proteau, I.G. Ganley, K. L. McPhail, J.E. Ishmael, Coibamide A induces mTOR-independent autophagy and cell death in human glioblastoma cells, *PLoS One* 8 (2013), e65250.
- [27] U. Ahumada-Castro, E. Silva-Pavez, A. Lovy, E. Pardo, J. Molgomicron, C. Cardenas, mTOR-independent autophagy induced by interrupted endoplasmic reticulum-mitochondrial Ca(2+) communication: a dead end in cancer cells, *Autophagy* 15 (2019) 358–361.
- [28] J. Kim, M. Kundu, B. Viollet, K.L. Guan, AMPK and mTOR regulate autophagy through direct phosphorylation of Ulk1, *Nat. Cell Biol.* 13 (2011) 132–141.
- [29] S. Missiroli, M. Bonora, S. Patergnani, F. Poletti, M. Perrone, R. Gafa, E. Magri, A. Raimondi, G. Lanza, C. Tacchetti, G. Kroemer, P.P. Pandolfi, P. Pinton, C. Giorgi, PML at mitochondria-associated membranes is critical for the repression of autophagy and cancer development, *Cell Rep.* 16 (2016) 2415–2427.
- [30] D. De Stefani, A. Raffaello, E. Teardo, I. Szabo, R. Rizzuto, A forty-kilodalton protein of the inner membrane is the mitochondrial calcium uniporter, *Nature* 476 (2011) 336–340.
- [31] N. Nemani, S. Shanmughapriya, M. Madesh, Molecular regulation of MCU: implications in physiology and disease, *Cell Calcium* 74 (2018) 86–93.
- [32] S. Pankiv, T.H. Clausen, T. Lamark, A. Brech, J.A. Bruun, H. Outzen, A. Overvatn, G. Bjorkoy, T. Johansen, p62/SQSTM1 binds directly to Atg8/LC3 to facilitate degradation of ubiquitinated protein aggregates by autophagy, *J. Biol. Chem.* 282 (2007) 24131–24145.
- [33] X. Zhang, Q. Cheng, H. Yin, G. Yang, Regulation of autophagy and EMT by the interplay between p53 and RAS during cancer progression (Review), *Int. J. Oncol.* 51 (2017) 18–24.
- [34] J. Miyazaki, K. Ito, T. Fujita, Y. Matsuzaki, T. Asano, M. Hayakawa, T. Asano, Y. Kawakami, Progression of human renal cell carcinoma via inhibition of RhoA-ROCK axis by PARG1, *Transl. Oncol.* 10 (2017) 142–152.
- [35] Y. Liu, X. Wang, G. Wang, Y. Yang, Y. Yuan, L. Ouyang, The past, present and future of potential small-molecule drugs targeting p53-MDM2/MDMX for cancer therapy, *Eur. J. Med. Chem.* 176 (2019) 92–104.
- [36] L. Morshaeuser, M. May, M. Burger, W. Otto, G.C. Hutterer, M. Pichler, T. Klatte, P. Wild, L. Buser, S. Brookman-May, p53-expression in patients with renal cell carcinoma correlates with a higher probability of disease progression and increased cancer-specific mortality after surgery but does not enhance the predictive accuracy of robust outcome models, *Urol. Oncol.* 36 (2018), 94 e15–94 e21.
- [37] G. Bousquet, M. El Bouchtaoui, C. Leboeuf, M. Battistella, M. Varna, I. Ferreira, L. F. Plassa, D. Hamdan, P. Bertheau, J.P. Feugeas, D. Damotte, A. Janin, Tracking sub-clonal TP53 mutated tumor cells in human metastatic renal cell carcinoma, *Oncotarget* 6 (2015) 19279–19289.
- [38] E. Tasdemir, M.C. Maiuri, L. Galluzzi, I. Vitale, M. Djavaheri-Mergny, M. D'Amelio, A. Criollo, E. Morselli, C. Zhu, F. Harper, U. Nannmark, C. Samara, P. Pinton, J. M. Vicencio, R. Carnuccio, U.M. Moll, F. Madeo, P. Paterlini-Brechot, R. Rizzuto, G. Szabadkai, G. Pierron, K. Blomgren, N. Tavernarakis, P. Codogno, F. Cecconi, G. Kroemer, Regulation of autophagy by cytoplasmic p53, *Nat. Cell Biol.* 10 (2008) 676–687.
- [39] F. Sakanashi, M. Shintani, M. Tsuneyoshi, H. Ohsaki, S. Kamoshida, Apoptosis, necroptosis and autophagy in colorectal cancer: associations with tumor aggressiveness and p53 status, *Pathol. Res. Pract.* 215 (2019) 152425.
- [40] K.L. Russell, C.M. Gorgulho, A. Allen, M. Vakaki, Y. Wang, A. Facciabene, D. Lee, P. Roy, W.J. Buchser, L.J. Appleman, J. Maranchie, W.J. Storkus, M.T. Lotze, Inhibiting autophagy in renal cell cancer and the associated tumor endothelium, *Canc. J.* 25 (2019) 165–177.
- [41] S. Yang, X. Wang, G. Contino, M. Liesa, E. Sahin, H. Ying, A. Bause, Y. Li, J. M. Stommel, G. Dell'antonio, J. Mautner, G. Tontonoz, M. Haigis, O.S. Shirihai, C. Doglioni, N. Bardeesy, A.C. Kimmelman, Pancreatic cancers require autophagy for tumor growth, *Genes Dev.* 25 (2011) 717–729.